Trends in Microfluidics with Complex Fluids

Thomas Pfohl, Frieder Mugele, Ralf Seemann, and Stephan Herminghaus*[a]

The rapid developments in biotechnology create a great demand for fluid handling systems on the nano- and picoliter scale. The characterization of minute quantities of DNA or protein samples requires highly integrated, automated, and miniaturized "total analysis systems" (μ-TAS). The small scales necessitate new concepts for devices both from a technological and from a fundamental physical point of view. Here, we describe recent trends in both areas. New technologies include soft lithography, chemical, and topographical structuring of surfaces in order to define pathways for liquids, as well as electrowetting for manipulation purposes. Fundamentally, the interplay between geometric confinement and the size of biological macromolecules gives rise to complex dynamic behavior. The combination of both fluorescence imaging and scattering techniques allows for detailed insight into the dynamics of individual molecules and into their self-assembly into supramolecular aggregates.

In recent years, remarkable progress has been achieved in biomedicine as well as in bioanalysis, such as the decoding of the human genome. The rapid and efficient analysis of even minimal sample volumes is a crucial requirement for this immense progress, which has only become possible by miniaturizing analysis systems. This is the main driving force for the continuous miniaturization of fluidic systems leading to the development of complete analytic systems of the size of a single chip ("micro-lab"). Miniaturized fluidic systems have several purposes, such as amplification, digestion, and analysis of deoxyribonucleic acid (DNA) sequences. Furthermore, they may be used to separate and analyze single defective cells in order to diagnose specific diseases at early stages. For the upcoming era after the sequencing of the genome, the analysis of gene and protein functions ("structural genomics" and "proteomics") creates a huge demand for advanced biotechnological systems.[1, 2] These systems can only be realized using miniaturized fluid handling systems, which allow the rapid and efficient analysis of structures and functions with minimal sample volume.

Due to the wide range of open questions, microfluidics has rapidly turned into an interdisciplinary research field equally including physics, chemistry, materials science, and engineering. Besides developing new materials for microfluidic applications as well as miniaturized devices, there are a number of fundamental physical problems related to fluid flow in such microsystems. The fluids of interest in biotechnology are by no means "simple liquids". In most cases, they are aqueous solutions containing long-chain macromolecules such as DNA or proteins. Frequently, the molecular dimensions are comparable to the dimensions of the channels in the microfluidic device. It turns out that the dynamic properties of long-chain macromolecules are different in such confining geometries compared to free macromolecules in a bulk solution. A detailed understanding of flow dynamics and molecular transport in micro- and nanostructures is thus needed.

However, the interest in dynamic processes with confined complex liquids goes beyond the technological aspects discussed above: Any process in living cells, such as intracellular material transport through the protein network of the cytoskeleton, involves the flow of complex liquids in complex geometries with characteristic length scales comparable to the size of the transported molecules.

In the following, we focus on a few specific examples, which illustrate the diversity of activities and some of the fundamental physical effects that are important to microfluidics. First, we describe a few applications of microfluidic devices in biotechnology. After that, we discuss a few technological aspects mainly related to the use of polymeric materials in device fabrication. Then, we discuss the so-called open microfluidic systems, which represent a new approach to microfluidics based on the presence of free liquid – vapor or liquid – liquid interfaces. Finally, we discuss the behavior of complex fluids in microsystems and a few studies from fundamental biophysical research.

Microfluidic Systems in Biotechnology

The driving force for the continuous miniaturization of flow systems in biotechnology and bioanalysis is not only the reduction of sample volumes down to nano- and picoliter sizes. Miniaturization also leads to remarkably improved performance,

[a] *Prof. Dr. S. Herminghaus, Dr. T. Pfohl, Priv. Doz. Dr. F. Mugele, Dr. R. Seemann*
Angewandte Physik, Universität Ulm
Albert-Einstein-Allee 11, 89069 Ulm (Germany)
Fax: (+49) 731-502-2958
E-mail: stephan.herminghaus@physik.uni-ulm.de

 DOI: 10.1002/cphc.200300847

such as higher separation efficiency, shorter analyzing times, and enhanced detection sensitivities. Integrated microfluidic devices containing pumps, valves, separation systems, and detectors follow the concept of the so-called total (chemical) analysis systems, TAS.[3] Ideally, each step of the analysis is realized on an integrated device (μ-TAS, "lab-on-a-chip"). The steps include sampling, sample pretreatment, (bio-) chemical reactions, separation, and their analytical identification. This concept was impressively realized for example, by a nanoliter-DNA-analysis system for amplification as well as digestion, separation, and identification of DNA sequences.[4] The device, 47 mm × 5 mm × 1 mm in size, integrates a nanoliter injector, mixer, temperature-controlled reaction chamber, a separation system based on electrophoresis gel, and a fluorescence detector. This analytical device was prepared on glass and silicon substrates using photolithography and wet chemical etching. All components except for the light source, the pressure supply, and the controlling circuit were placed on the chip.

Bioanalysis applications often deal with large macromolecules, which hardly pass through conventional polyacrylamide or agarose electrophoresis gels due to the restricted mesh size of the gel matrix. To overcome this drawback, artificial structures with dimensions larger than the mesh sizes of the gels have been fabricated. Using lithographically microstructured channel systems, it was possible to separate DNA macromolecules of high molecular weight.[5] Such electrophoresis channels consist of alternating wide and narrow areas (Figure 1), the narrow ones

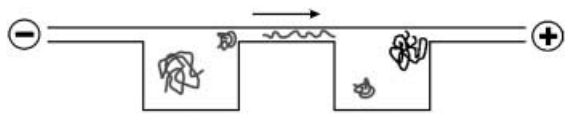

Figure 1. Electrophoretic DNA separation based on lithographically microstructured channels of alternating wide and narrow areas.[5]

having a depth of only about 100 nm. This is less than the typical extension of the random coil conformation of long DNA macromolecules in aqueous solution. The transition rate from the wider to the narrower regions of the channel depends on the length of the molecules. Therefore, the drift velocity in the electrophoresis field also depends on the molecular weight and thus allows for separation. This new microelectrophoresis system was realized on a device 15 mm long and shows a ten-times faster separation than conventional standard gel electrophoresis. Furthermore, the costly loading of the microchips with electrophoresis gels is omitted.

Technological Aspects

For the fabrication of microfluidic systems, a large number of concepts have been developed. Although the first microfluidic devices were made of silicon or glass, using conventional methods known from microelectronics (photolithography and subsequently dry or wet etching), nowadays polymeric devices are used more and more due to their low production cost and their flexibility for applications. The so-called soft lithography is a new and easy-to-use method for the fabrication of prototypes and specific microfluidic systems.[6] Soft lithography is a microstructuring technique based on the printing and molding of elastic polymers. Most commonly, the silicone elastomer PDMS (crosslinked polydimethyl siloxane) is used because of its advantageous properties: It is inexpensive, nontoxic, chemically inactive, and mechanically flexible. Sealing with glass, silicon, or additional PDMS substrates may be achieved by oxidizing the PDMS surface. In Figure 2, the typical preparation steps of a microfluidic device made of PDMS are illustrated. By using photolithography, a relief structure is transferred onto a photoresist-coated silicon or glass substrate. For the preparation of PDMS casts, the photoresist structures may be directly used as masks. The photoresist mask is filled with PDMS, which is then crosslinked. A single mask allows the preparation of several PDMS casts. After releasing the PDMS cast, tubing is connected to the device. Using oxygen plasma, the surface of the PDMS cast is oxidized. Subsequently, it is brought into contact with glass, silicon, or additional PDMS surfaces for covalent binding. A

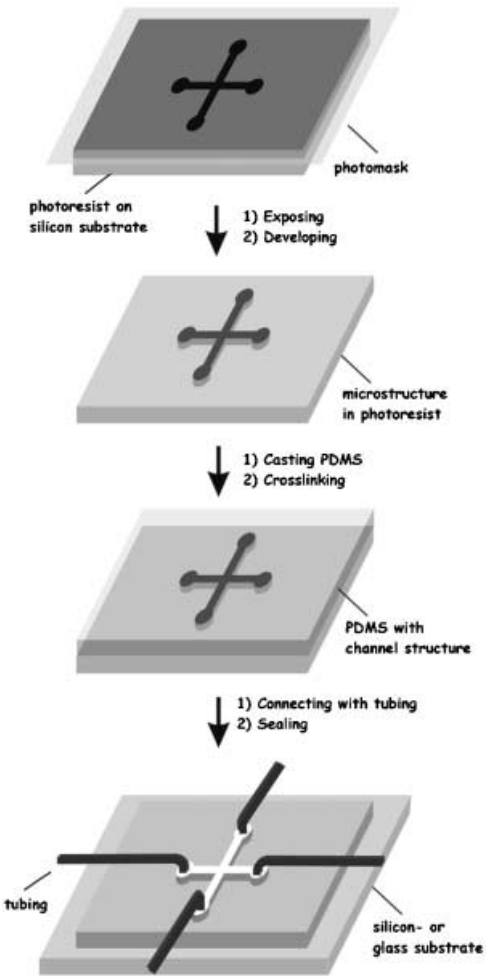

Figure 2. Illustration of the typical preparation steps of microfluidic devices made of PDMS.

device thus sealed withstands pressures of 5 – 10 bar. This new class of processes also allows the preparation of three-dimensional channel networks containing pumps and valves made of elastic polymer materials.[7, 8]

Liquid Flow in Microchannels

The flow behavior of liquids in microchannels is characterized by the Reynolds number $Re = v l \rho / \eta$, where v is the flow rate, l is the typical spatial dimension of the system (for example, the channel width), ρ is the mass density of the liquid, and η is its dynamic viscosity.[9] Due to the small dimensions of microfluidic devices and typical flow velocities of a few millimeters per second, Re is rarely larger than one. Since turbulence does not appear below $Re \approx 10^3$, inertia effects may be neglected and the flow in microfluidic devices is always laminar. In this case, the flow may be described by the following approximation: $\eta \Delta v = \mathrm{grad}\, p$, where p is the pressure field. Inside long and narrow microchannel geometries, the velocity field is parallel to the local orientation of the channel walls and the pressure decreases in the longitudinal direction. This gives rise to a parabolic velocity profile (the Poiseuille profile). Conventionally, it is assumed that the flow velocity vanishes at the channel walls (no-slip boundary condition). The momentum, mass, and the heat transfer perpendicular to the flow direction are controlled by diffusion and thermal conduction. However, due to the small dimensions, deviations from this standard hydrodynamic textbook behavior sometimes appear. For instance, the friction of the liquid at the channel walls may be highly complicated. The classical, no-slip boundary condition was found to be violated in a variety of systems. Slippage was found to depend critically on surface roughness, on the liquid – substrate interaction, and on the rheological properties of the fluid.[10, 11]

If parabolic flow profiles, which are characteristic for pressure-driven flows, are used for the separation of different molecules, the bands of distinct species are broadened. Therefore, it is desirable to minimize the variation of the flow velocity across the channel. Ideally, one would like to obtain a pluglike flow profile. This may be achieved by electro-osmosis. Electro-osmosis, which may be applied to water or other very polar solvents, makes use of the inhomogeneous charge distribution near the channel walls due to the preferential adsorption of one ionic species. An electrical field applied along the channel axis creates a net force on the diffuse counter ion layer that screens immobile surface-adsorbed ions. Hence, the liquid inside the channel is driven by a force that acts only on its boundary. As a result, the electro-osmosis-driven flow has an almost homogeneous velocity profile.[6] Another possibility for avoiding broadening is making use of complex fluid flow. This involves localizing reagents inside droplets surrounded by an immiscible fluid such as air or oil.[4, 12, 13]

Open Microfluidic Systems

The microfluidics devices described so far have consisted of channels, reservoirs, and so on, embedded into a solid matrix. Alternatively, it is also interesting to consider systems with free liquid – liquid or liquid – vapor interfaces. In this approach, which we like to term "open microfluidics", fluid microstructures are prepared and manipulated on top of single, freely accessible surfaces. There are essentially two different strategies to define the positions of channels, reservoirs, and so on, where the fluid is supposed to flow. The first one is to prepare chemical wettability patterns on a planar substrate. Since the liquids in microfluidics applications are typically aqueous solutions, pathways for the liquid consist of hydrophilic areas within an otherwise hydrophobic surface. Such chemical patterns can be prepared by various techniques, including, for instance, conventional photolithographic and microcontact printing. Figure 3 shows cylindrical sections of water condensed onto hydrophilic stripes upon cooling under the dew point.[14]

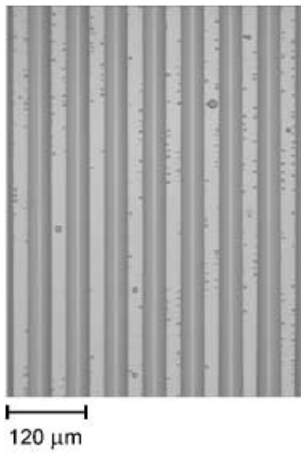

Figure 3. Water condensed onto hydrophilic stripes upon cooling under the dew point, on an otherwise hydrophobic substrate (MgF_2 stripes on PDMS). The liquid spontaneously formed parallel channels.

The second strategy to control the liquid is to pattern the surface topography. This relies on the fact that liquids prefer to wet wedges and grooves as compared to planar surfaces—provided that the intrinsic contact angle is sufficiently small. For instance, wedge-wetting is known to occur in rectangular grooves below a critical angle of 45°. In general, a rich variety of stable liquid morphologies can be created, depending on the contact angle and geometric details, such as, the aspect ratio of the grooves (see Figure 4). One particularly attractive aspect of liquid condensates in wedges or grooves is that their surface can have a negative mean curvature.[15] This allows for stabilization of liquid structures in contact with large reservoirs at zero Laplace pressure, or in the presence of vapor close to saturation. Even more flexible ways of generating complex fluid microstructures can be envisioned if one combines topographical and chemical wettability patterns.

There is one difficulty with open microfluidic systems, which is intimately related to the presence of free liquid – vapor or liquid – liquid interfaces: Due to interfacial tension, only interface morphologies with a constant mean curvature are mechanically stable. If, for instance, we connect two droplets of different size via a liquid channel, we observe that the smaller one is

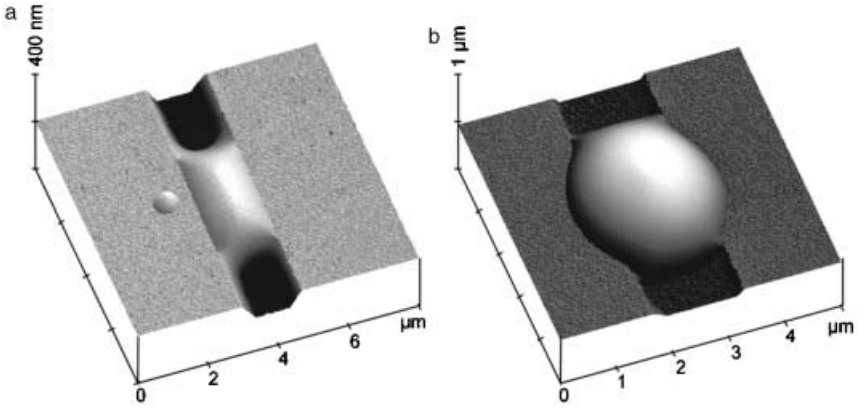

Figure 4. AFM images of liquid structures on a silicon substrate with etched grooves. The contact angle of the substrate was varied by decorating the silicon surface with different self-assembly monolayers. a) Aspect ratio (depth/width) a = 0.07, contact angle θ = 22°; the liquid droplet confined in the groove has positive mean curvature and coexists with wedge-wetting along the lower corners of the groove. b) a = 0.07, θ = 50°; the liquid droplet is not confined in the groove and extends over the plateaus.

immediately "eaten up" by the larger one, due to the difference in Laplace pressure (Figure 5) $\Delta P_L = \sigma/2(1/r_1 - 1/r_2)$. Dynamic instabilities occur unless the mean curvature is constant. Furthermore, the second variation of the free energy with respect to the shape must be positive. This constraint greatly limits the class of morphologies eligible for applications in open microfluidic systems.

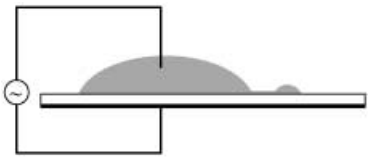

Figure 5. Two liquid droplets connected by a channel (gray) on an insulating substrate with a submersed counter electrode. In electrowetting experiments, a voltage (AC or DC) is applied between the liquid (for example, via an immersed Pt wire) and the counter electrode.

Recently, however, we were able to show that electric fields can be used to overcome this problem.[16] If we apply an electrostatic potential to the structure sketched in Figure 5, there is a geometry-dependent electric field distribution $E(r)$ outside the liquid. Inside the liquid the field vanishes, provided the material is sufficiently conductive. The latter is not a serious limitation for typical buffer solutions in biological applications. In this case, the discontinuity of the electric field gives rise to an electrostatic pressure $p_{el} = -\varepsilon_0/2E^2$ acting on the surface, where ε_0 is the absolute dielectric constant. The negative sign indicates that the pressure is opposed to the Laplace pressure, that is, it tends to increase the droplet volume. In order to understand how the electric pressure stabilizes the smaller droplet with respect to the larger one, we assume that the field distribution around each droplet is the same as in a spherical capacitor, that is, $E(r) \sim 1/r^2$. If we now allow for material exchange between the two droplets, we note that the electric pressure in the small droplet is much larger than in the larger one. Furthermore, it diverges faster than the Laplace pressure as $r \rightarrow 0$. Hence, suitable electric field configurations can be used to stabilize complex fluid microstructures if their surface mean curvature is not constant. Figure 6 shows an experimental realization of this situation, where the small droplets could indeed be stabilized with respect to the large reservoir. In the experiments shown in Figure 6, an electric potential was applied between the liquid and a counter electrode located underneath the thin insulating substrate.

In addition to the electrostatic stabilization of complex fluid microstructures just described, this geometry gives rise to another interesting phenomenon, the so-called electrowetting effect. Electrowetting amounts to the fact that the contact angle

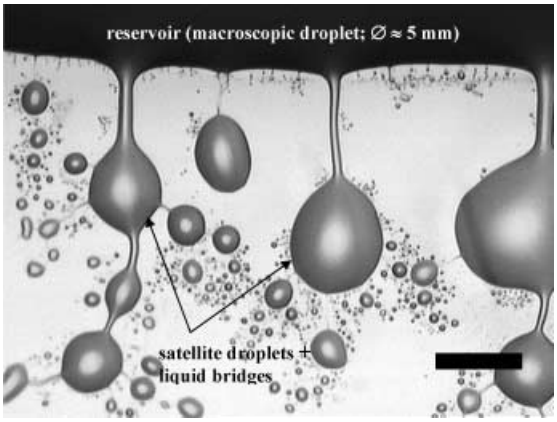

Figure 6. Electrostatically stabilized configuration of liquid microdroplets (glycerol) connected to a large reservoir (scale bar: 50 µm).

θ of conductive liquids can be reduced by applying a voltage. If the substrate consists of an insulating layer of thickness d and dielectric constant ε with an underlying counter electrode, the contact angle variation is described by the so-called Lippmann equation, Equation (1).[17]

$$\cos\theta(U) = \cos\theta(0) + \varepsilon\varepsilon_0 U^2/2\gamma d \quad (1)$$

where U is the voltage applied between the counter electrode and the liquid. For practical purposes, one can say that the applied voltage leads to an increase of the solid–liquid interfacial tension. Because of the efficiency, the high switching rate, and the ease with which electric fields can be applied, electrowetting has become one of the most popular strategies for manipulating liquid microstructures on solid surfaces. Manipulation is typically achieved by patterning the counter electrodes. If suitable voltages are applied to different sections of the counter electrodes, liquid microstructures can lower their free energies by deforming or moving towards the electrode

with the highest voltage. Besides moving droplets on planar substrates, electrowetting is also used to manipulate capillary bridges between two opposing planar surfaces.[18] Furthermore, since the wetting of topographic structures is particularly sensitive to the contact angle, it appears promising to combine electrowetting with, for example, the wedges and grooves discussed above. The potential of this combination remains to be explored.

One of the prominent problems in microfluidics is mixing. Due to the small dimensions of microfluidic devices, turbulence, which is the basis for mixing in macroscopic fluid handling systems, is usually absent. In the specific case of microfluidic capillary bridges, the electrowetting effect again provides an interesting approach. It turns out that, if the (AC) voltage and the separation of the surfaces (with respect to the liquid volume) are chosen correctly, the liquid can be forced into a mode where it oscillates periodically between the capillary bridge state and a state of two separated droplets (see Figure 7).[18] The occurrence of this mode can be explained by considering the destabilizing effect of electrowetting on the capillary bridge, and the destabilizing effect of the mutual electrostatic attraction between the surfaces of the two separated droplets, respectively. The rapid formation and rupture of the capillary bridge, however, involves highly nonlinear dynamic flow patterns that are expected to promote mixing.

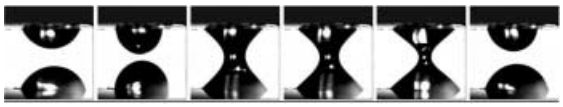

Figure 7. Oscillating capillary bridge (glycerol – water mixture) between two electrowetting substrates. For suitable combinations of applied voltage and substrate separation, bridges break and reform periodically (rate $\approx 1\ s^{-1}$).[18] At high voltage, the bridge state is destabilized by electrowetting. Simultaneously, the state consisting of two separated droplet states is destabilized by their mutual electrostatic attraction. (droplet diameter: ≈ 1 mm; video sequences can be downloaded at www.wetting.de/electrowetting.htm)

Complex Fluids in Microstructures

As already mentioned, the fluids of interest in biotechnological applications may not be described as "simple liquids". Therefore, finite size effects become relevant for the flow dynamics in miniaturized flow systems. Such effects may be demonstrated by the dynamic properties of larger chain molecules in confining geometries, which clearly differ from their molecular behavior in "free volume". An excellent model macromolecule for studying the influence of confinement on the dynamics of molecular properties is the cytoskeletal protein actin. Actin belongs to the proteins of intracellular filamentous networks. It is possible to detect single actin filaments (diameter: about 10 nm, length: several μm) by fluorescence labeling. Furthermore, actin filaments can be polymerized in a cell-free medium. Filaments, being much shorter than the persistence length of about 17μm, behave as rodlike molecules, whereas longer filaments ($\gg$ 17μm) show a flexible behavior. These regimes, including the intermediate semiflexible regime, which reasonably is described by the "wormlike chain" (WLC) model,[19] can be studied using fluorescence microscopy. Since typical molecular bending energies are in the range of the thermal energy, single filaments show random fluctuations similar to Brownian motion (Figure 8). When these filaments are confined in microchannels of different widths (depth $\sim$3μm), an elongation of the actin filaments can be observed, as a function of the channel width (Figure 9).[20] The filaments fluctuate around their elongated conformation and the mean end-to-end distance increases with decreasing channel width.

Figure 8. Fluctuations of a single, fluorescently labeled actin filament in a cell-free media (time interval $\Delta t = 5$ s).

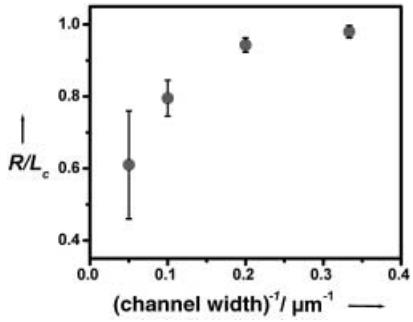

Figure 9. Influence of confinement on the elongation of single actin-filaments: increase of the ratio of the end-to-end distance (R) to the contour length with decreasing channel width.

Besides the stiff actin filaments, more flexible macromolecules having a contour length in the range of the channel width, such as DNA, are also strongly influenced by confinement.[21] For example, DNA molecules in semidilute solutions (larger than 10 mg mL^{-1}) may be oriented parallel to the channel direction. Due to the birefringence of the molecules, the net molecular alignment can be visualized by polarization microscopy (Figure 10). If the contour length of the DNA strands is smaller than the channel width, no preferential orientation is observed. The confinement of macromolecular materials that usually form two-dimensional liquid crystalline-like structures leads to highly ordered systems, which allows direct structural characterization using X-ray microdiffraction methods without the

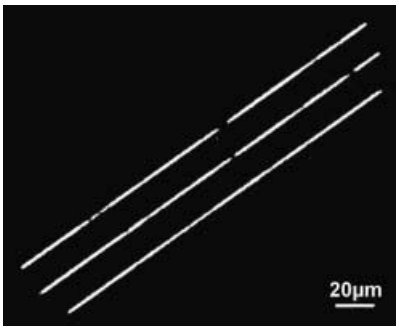

Figure 10. Polarization microscopy image of three microchannels filled with DNA. The DNA molecules show a preferential orientation along the channels.

complications introduced by powder averaging in nonoriented samples.[22]

Materials consisting of smaller molecules that are able to form liquid crystalline phases are also strongly affected by geometric constraints.[21] Figure 11 (top) shows an example: the microscopic domain structure of the smectic liquid crystal 8CB (4′-*n*-ocytl-4-cyanobiphenyl; molecular length about 3 nm) is clearly

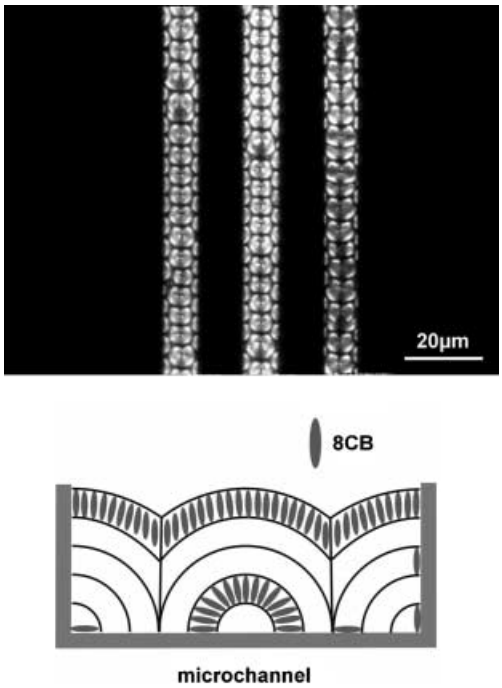

Figure 11. Top: Polarization microscopy image of microchannels filled with the smectic liquid crystal 8CB (smectic A).[21] The texture results from different orientations of the birefringent liquid crystalline layers in the microchannels. Bottom: Sketch of the layer structure of the confined liquid crystal molecules (side view). The structure is determined by the different orientation of the liquid crystal at the interfaces to air and to the walls, as well as by the geometric constraints of the microchannels.

determined by the geometry of the microchannels, although the molecular lengths of the liquid crystals are several orders of magnitude smaller than the dimensions of the channels. The liquid crystal molecules have a different orientation at the 8CB/air interface (perpendicular to the interface) and at the 8CB/channel walls (parallel to the walls; Figure 11, bottom). It is, thus, the combination of incompatible boundary conditions with geometric confinement that gives rise to the textures observed in polarization microscopy.

Fundamental Research with Microfluidic Devices

The influence of simple geometric constraints on the flow behavior of complex liquids may be used for fundamental experiments, in biophysics or polymer physics. Frequently used microfluidic devices consist of two crossed channels.[23] As shown in Figure 12, such an arrangement allows the

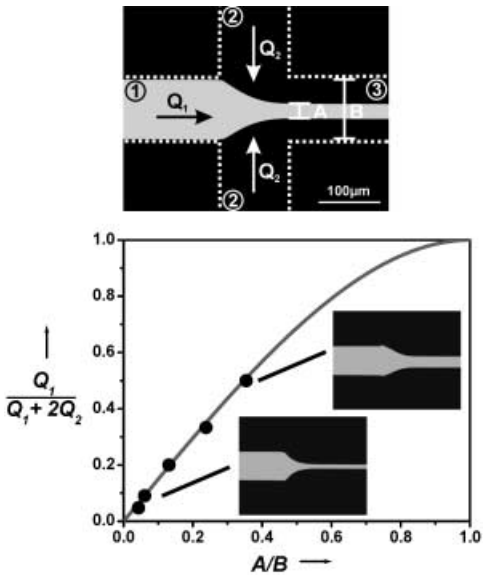

Figure 12. Top: Hydrodynamic focusing of a fluorescein solution imaged by fluorescence microscopy. The channel walls are indicated by broken lines. Bottom: Ratio of the flow of the inlet channel 1 to the total flow as a function of the width of the focused liquid stream. The width of the stream can be controlled by the relative flow rates. The line can be obtained, if a Poiseuille-profile in channel 3 is taken into account.

hydrodynamic focusing of a liquid jet in the microstructure, which opens up a wide field of experiments. Figure 12, top, shows the hydrodynamic focusing of an aqueous solution containing fluorescein. The stream containing fluorescently labeled water in the inlet channel appears green and is squeezed into a thin jet by the streams from the two side channels containing nonlabeled water. The width of the jet may be adjusted by the ratio of the flow rates Q_1 of the inlet channel (channel 1) and Q_2 of the side channels (channels 2) and, remarkably, may become smaller than the actual channel width (Figure 12, bottom).

Such a device allows diffusive mixing and the examination of any reactions if the solutions in the inlet channel and the side channels contain different reactants. The inlet and side solutions flow side by side (laminar flow). At the interface, the reactants are mixed due to molecular diffusion, whereby the reaction is initiated. The mixing time can be controlled by the width of the

focused jet, depending on the diffusion time of molecules from the side flow across the inlet stream. If jet streams with a width of about 50 nm are formed, the diffusive mixing time is reduced to less than 10μs.[23] The time evolution of the reaction is separated spatially in steady-state flow. Apart from the excellent time resolution, this method consumes small sample volumes. This is particularly important in the field of biomaterials, since they are only available in minute quantities.

Using this fascinating method, Pollack et al. succeeded in examining the early steps of protein folding,[24] as well as the folding of ribonucleic acid (RNA)[25] by means of small angle X-ray scattering. Folding was initiated by adding folding-inducing reactants in the side streams. The evolution of the folding processes could be observed with a time resolution of sub-milliseconds. In a different small angle X-ray experiment, the flow behavior of a smectic liquid crystal in such a microfluidic device (inlet channel: 8CB; side channels: water) was investigated by scanning a microfocused X-ray beam.[26] A monochromatic X-ray beam was focused down to about 5μm by a Fresnel-zone plate to image the structure and orientation of the liquid crystal in this device with a spatial resolution of a few micrometers. The alignment of (biological) liquid crystals due to the elongational flow in the hydrodynamically focused jet allows the direct observation and characterization of assemblies of oriented supramolecular materials.

The microfluidic device shown in Figure 13 may also be used for single molecule investigations. When channels 1 and 3 are used as the inlet channels for continuous liquid streams (outlet: the side channels), with the same average flow velocity, it is possible to create a hyperbolic flow profile having a stagnation point in the center of the intersection (Figure 13).[27] If a chainlike macromolecule is present at this stagnation point, its conformation may be changed from a random coil into an elongated shape due to the spatially homogeneous velocity gradient. In doing so, it was possible to study the influence of the elongational flow of the solvent on the conformation of single macromolecules of fluorescently labeled λ-bacteriophage-DNA by means of fluorescence microscopy. The stretching rate of individual macromolecules is highly variable and depends on the conformation that develops during elongation. The variability of shapes of stretched macromolecules (for example, dumbbell, folded, kinked) is due to the dependence of dynamic evolution on the initial conformation. Not only the dynamics, but also the final stages of the stretching of individual macromolecules differ largely, depending on the initial equilibrium conformation. Even at the highest strain rates, only the macromolecules are stretched to their complete contour length. In comparison to classical "bulk" measurements on polymer deformation, which are averaged over a macroscopic number of macromolecules and show a discrete coil to stretch transition at a critical flow rate, single polymers do not undergo collective and simultaneous unwinding.

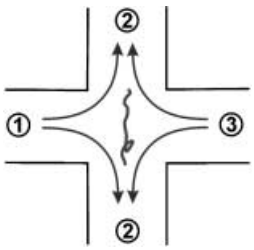

Figure 13. *Sketch of the hyperbolic flow profile in crossed microchannels.[27] The elongation of a single DNA molecule is also indicated.*

Future Flow Directions

The studies on microfluidic devices described herein just give a faint idea of what may be expected from future experiments. Decreasing the channel dimensions to the nanometer range, or using more complicated device geometries, will give access to new and fascinating effects. Additionally, miniaturization, a combination of techniques such as electrowetting and soft lithography, and the extension to three dimensions will lead to a new class of "stand alone" labs on a chip. Although the technical developments of microfluidic systems are mainly determined by applications in bioanalysis, it is expected that completely new applications will emerge in the future. The development of microfluidic assembly lines for the preparation of new "smart materials" is now under discussion. An integration of microfluidics with "molecular nanomachines" (such as actin/myosin or tubelin/kinesin), which have been optimized by nature, is conceivable. It may be possible to machine "molecular cyborgs" by self-assembly of biomaterials and inorganic microsystems: highly integrated hybrid systems, which may be incorporated into blood vessels to fulfill highly specific functions. In comparison to conventional top-down approaches, such systems would come along with elegant natural repairing mechanisms—an important property, the lack of which has limited the success of many artificial nanomachines so far.

Acknowledgements

We thank Myung Chul Choi, Ulrike Ciesla, Hartmut Gau, Anke Klingner, Sarah Köster, Youli Li, Renate Nikopoulos, Alexander Otten, and Cyrus R. Safinya. T.P. thanks the German Science Foundation (DFG) for support within the Emmy-Noether Program. S.H. and F.M. thank the DFG for various grants within the priority program "Wetting and Structure Formation at Interfaces".

Keywords: biophysics · microfluidics · microreactors · nanotechnology · proteomics

[1] M. Gerstein, N. Jing, R. Jansen, *Science* **2002**, *295*, 284.
[2] G. T. Montelione, *Proc. Natl. Acad. Sci. USA* **2001**, *98*, 13488.
[3] S. C. Jakeway, A. J. de Mello, E. L. Russell, *Fresenius J. Anal. Chem.* **2000**, *366*, 525.
[4] M. A. Burns, B. N. Johnson, S. N. Brahmasandra, K. Handique, J. R. Webster, M. Krishan, T. Sammarco, P. M. Man, D. Jones, D. Heldsinger, C. H. Mastrangelo, D. T. Burke, *Science* **1998**, *282*, 484.
[5] J. Han, H. G. Craighead, *Science* **2000**, *288*, 1026.
[6] G. M. Whitesides, A. D. Stroock, *Phys. Today* **2001**, *June*, 42.

[7] M. A. Unger, H.-P. Chou, T. Thorsen, A. Scherer, S. R. Quake, *Science* **2000**, *288*, 113.
[8] R. H. Liu, M. A. Stremler, K. V. Sharp, M. G. Olsen, J. G. Santiago, R. J. Adrian, H. Aref, D. J. Beebe, *J. Microelectromech. Syst.* **2000**, *9*, 190.
[9] E. Guyon, J.-P. Hulin, L. Petit, C. D. Mitescu, *Physical Hydrodynamics*, Oxford University Press, Oxford, **2001**.
[10] V. S. J. Craig, C. Neto, D. R. M. Williams, *Phys. Rev. Lett.* **2001**, *87*, 054504.
[11] Y. Zhu, S. Granick, *Phys. Rev. Lett.* **2001**, *87*, 096104.
[12] K. Handique, M. A. Burns, *J. Micromech. Microeng.* **2001**, *11*, 548.
[13] H. Song, J. D. Tice, R. F. Ismagilov, *Angew. Chem.* **2003**, *115*, 792; *Angew. Chem. Int. Ed.* **2003**, *42*, 768.
[14] H. Gau, S. Herminghaus, P. Lenz, R. Lipowsky, *Science* **1999**, *283*, 46.
[15] R. Seemann, M. Brinkmann, F. Lange, E. Kramer, R. Lipowsky, unpublished results.
[16] F. Mugele, S. Herminghaus, *Appl. Phys. Lett.* **2002**, *81*, 2303.
[17] C. Quilliet, B. Berge, *Curr. Opin. Colloid Interface Sci.* **2001**, *6*, 1.
[18] A. Klingner, S. Herminghaus, F. Mugele, *Appl. Phys. Lett.* **2003**, *82*, 4187.
[19] O. Kratky, G. Porod, *Recl. Trav. Chim. Pays-Bas* **1949**, *68*, 1106.
[20] a) S. Köster, A. Otten, M. C. Choi, Y. Li, C. R. Safinya, T. Pfohl, unpublished results; b) S. Köster, Diploma thesis, University of Ulm, **2003**.
[21] T. Pfohl, J. H. Kim, M. Yasa, H. P. Miller, G. C. L. Wong, F. Bringezu, Z. Wen, L. Wilson, Y. Li, M. W. Kim, C. R. Safinya, *Langmuir* **2001**, *17*, 5343.
[22] G.-C. L. Wong, Y. Li, I. Koltover, C. R. Safinya, Z. Cai, W. Yun, *Appl. Phys. Lett.* **1998**, *73*, 2042.
[23] J. B. Knight, A. Vishwanath, J. P. Brody, R. H. Austin, *Phys. Rev. Lett.* **1998**, *80*, 3863.
[24] L. Pollack, M. W. Tate, A. C. Finnefrock, C. Kalidas, S. Trotter, N. C. Darnton, L. Lurio, R. H. Austin, C. A. Batt, S. M. Gruner, S. G. J. Mochrie, *Phys. Rev. Lett.* **2001**, *86*, 4962.
[25] R. Russell, I. S. Millett, M. W. Tate, L. W. Kwok, B. Nakatani, S. M. Gruner, S. G. J. Mochrie, V. Pande, S. Doniach, D. Herschlag, L. Pollack, *Proc. Natl. Acad. Sci. USA* **2002**, *99*, 4271.
[26] B. Stuth, A. Snigirev, O. Konolov, A. Otten, R. Gauggel, T. Pfohl, *Proceedings for SRI 2003* **2003**, in press.
[27] D. E. Smith, S. Chu, *Science* **1998**, *281*, 1335.

Received: May 12, 2003 [C847]

